NACA RM E53D22

NACA

RESEARCH MEMORANDUM

ALTITUDE PERFORMANCE INVESTIGATION OF A HIGH-TEMPERATURE AFTERBURNER

By S. C. Huntley, Carmon M. Auble, and James W. Useller

Lewis Flight Propulsion Laboratory
Cleveland, Ohio

NATIONAL ADVISORY COMMITTEE FOR AERONAUTICS

WASHINGTON

June 26, 1953

NATIONAL ADVISORY COMMITTEE FOR AERONAUTICS

RESEARCH MEMORANDUM

ALTITUDE PERFORMANCE INVESTIGATION OF A HIGH-TEMPERATURE AFTERBURNER

By S. C. Huntley, Carmon M. Auble, and James W. Useller

SUMMARY

An investigation was conducted to ascertain the operational limits of a high-temperature afterburner and to determine its performance over a wide range of flight conditions. Operational limits were obtained at a flight Mach number of 0.8 and performance data were obtained at altitudes from 10,000 to 55,000 feet and flight Mach numbers from 0.6 to 1.0.

A combustion temperature of 3900° R at a combustion efficiency of 0.96 and a corresponding net thrust ratio of 2.03 was obtained for an altitude of 25,000 feet and a flight Mach number of 0.92. Peak combustion temperatures were obtained at the stoichiometric fuel-air ratio or at slightly richer mixtures. Maximum combustion efficiency was reached at a fuel-air ratio of about 0.055 and remained relatively constant with increasing fuel-air ratio. The importance of providing a good fuel distribution by using a large number of injection points rather than relying on penetration was demonstrated by the high burner performance. At the high exhaust-gas temperatures obtained, an excessive amount of air was required to cool the afterburner by the convective shell-cooling method used. As much cooling air as 34 percent of the exhaust-gas flow was required to maintain an average afterburner shell temperature of 1300° F at a combustion temperature of about 3600° R. These requirements stressed the need for a more effective method of utilizing the cooling air for high-temperature afterburners.

INTRODUCTION

The need of military aircraft for greater acceleration rates and higher flight speeds is demanding a more complete exploitation of the thrust potentialities of afterburners. In most previous investigations of afterburning conducted at the NACA Lewis laboratory, the maximum thrust potential of an afterburner was compromised to some extent by afterburner shell cooling. Burning was concentrated in the central portion of the afterburner and the unburned gases in the tail pipe surrounding the high-temperature region were used as a means of

minimizing the secondary air flow required to cool the afterburner shell. The net result was a mean bulk gas temperature somewhat below the maximum that might be expected for a homogeneous stoichiometric fuel-air mixture.

In response to the ever-increasing need for high thrust augmentation, an investigation was conducted that had as its primary objective the attainment of maximum exhaust-gas temperature and thrust (ref. 1). The afterburner shell was supplied with sufficient cooling from an external source to permit high-temperature operation. Performance approaching theoretical values was obtained at a nominal burner inlet pressure of 2450 pounds per square foot by the use of adequate flame-holder blockage, long fuel-mixing length, and relatively low burner-inlet velocity, and by careful matching of the fuel injection pattern to the gas flow pattern to obtain a uniform fuel-air ratio distribution.

Although the afterburners of reference 1 were capable of operation at exhaust-gas temperatures near theoretical, operational limits were not established and performance was obtained for only a limited range of flight conditions. The investigation reported herein was therefore conducted to ascertain the operational limits of the most promising high-temperature afterburner design of reference 1 and to determine its performance over a wide range of flight conditions.

An engine with the aforementioned afterburner was installed in an altitude test chamber at the NACA Lewis laboratory. Operational limits were obtained for a flight Mach number of 0.8 and performance characteristics were determined for a range of altitudes from 10,000 to 55,000 feet and flight Mach numbers from 0.6 to 1.0, which correspond to burner-inlet pressures from 510 to 3090 pounds per square foot. Efforts to further improve the performance of the afterburner led to a brief evaluation of the effect of fuel distribution and certain measurements of the fuel-air ratio distribution within the burner. The cooling requirements of the afterburner were also briefly evaluated.

APPARATUS

Engine

The axial-flow type turbojet engine used in this investigation (fig. 1) develops 3000 pounds thrust at static, sea-level conditions while operating at a rated engine speed of 12,500 rpm with an average turbine-outlet gas temperature of 1625° R. The air flow at this condition is about 58 pounds per second. The engine components consisted of an 11-stage axial-flow compressor, a compressor-outlet mixer, a double-annulus through-flow type combustor that merges into a single annulus, and a two-stage axial-flow turbine. The compressor-outlet mixer is used to obtain a velocity profile entering the combustor that provides a satisfactory radial temperature distribution at the turbine.

Afterburner

The afterburner configuration used in this investigation was similar to the most promising configuration developed in reference 1 and designated therein as the series C afterburner with the number 4 flame holder and corresponding optimized fuel pattern. The components of the afterburner consisted of a diffuser section, a combustion chamber with variable-area exhaust nozzle, a fuel distribution system, and a flame holder. Vortex generators were used on the inner cone at the diffuser inlet to minimize flow separation. The general arrangement and detailed dimensions of the afterburner shell and cooling shroud are shown in the sectional view of figure 2. Most of the afterburner combustion-chamber shell was provided with a uniform 1/2-inch annular passage for external air cooling while the exhaust nozzle and nozzle transition sections were water cooled. The required coolants were supplied from an outside source.

The fuel distribution system was installed in the diffuser section approximately 18 inches upstream of the flame holder. A total of 24 spray bars were equally spaced around the circumference of the afterburner, 12 long and 12 short tubes in alternate positions as sketched in figure 3. The spray bars were constructed of 1/4-inch Inconel tubing flattened to a thickness of about 1/8-inch. Holes of 0.020 inch diameter were drilled in the flattened sides of the spray bars, thus injecting fuel normal to the direction of gas flow. For a part of this investigation at high altitude only the 12 long spray bars were used. The 12 short spray bars were not removed but were separated from the fuel supply and blocked off.

The flame holder was of the three-ring V-gutter type with a blocked area of 35 percent. Details of the flame holder are shown in figure 4.

Ignition of the afterburner was accomplished by the hot-streak method wherein additional fuel was momentarily introduced at one location in the engine combustor to provide a flame through the turbine.

Installation

The engine and afterburner were installed in a 10-foot diameter altitude test chamber. A bulkhead in the test chamber, installed at a section corresponding to the engine inlet, was used to separate the inlet air flow from the exhaust gases and provide a means of maintaining a pressure differential across the engine. The exhaust gas from the jet nozzle was discharged into an exhaust diffuser. The pressure recovery in this diffuser was utilized to extend the maximum altitude limits of the facility. Combustion in the afterburner was observed through a periscope located in the exhaust duct behind the engine.

Instrumentation

Pressures and temperatures were measured at several stations throughout the engine and afterburner as indicated in figure 1. Air flow was determined from measurements of pressure and temperature at station 1. Afterburner-inlet conditions were determined from a comprehensive survey of pressure and temperature at the turbine outlet, station 5. The combustion temperature and thrust were determined from a survey of pressure at station 8 using a water-cooled rake located in a water-cooled section of constant diameter. For a part of the investigation the water-cooled rake was used to obtain samples of exhaust gas which were analyzed with an NACA mixture analyzer (ref. 2) to determine the fuel-air ratio distribution in the afterburner. Exhaust pressure was measured on the outside of the nozzle and in the plane of the exhaust-nozzle exit. Fuel flow was measured by means of a direct-reading calibrated rotameter.

Afterburner-shell temperatures were obtained with 6 thermocouples installed at each of two stations 6 inches apart located near the rear of the air-cooled portion of the afterburner shell. Cooling-air flow was measured using an orifice located in the supply line. Cooling-air temperatures were obtained from thermocouples located in plenum chambers at the inlet and outlet of the cooling passage.

PROCEDURE

Operational limits and performance at each flight condition were obtained by varying the afterburner fuel flow and jet-nozzle area while maintaining rated engine speed and the rated afterburner-inlet (turbine-outlet) temperature of 1625° R. Operational limits were obtained over a range of altitudes at a flight Mach number of 0.8. The lean fuel-air ratio limit was established by incipient blow-out observed through the periscope. The rich limit of operation was reached where the afterburner-inlet temperature was at the limiting or rated value with a wide open jet nozzle. Afterburner performance was obtained at altitudes from 10,000 to 55,000 feet and at flight Mach numbers of 0.6 to 1.0, thus covering a range of afterburner-inlet pressures of 510 to 3090 pounds per square foot. Inlet conditions to the engine at each flight condition corresponded to NACA standard atmosphere with 100 percent ram pressure recovery. Adequate cooling air and water were supplied to the afterburner shell from an external source to maintain the afterburner-shell temperature below 1550° F.

The symbols and method of calculating various parameters used in this report are shown in the appendix. The fuel used in the engine was clear unleaded gasoline (62 octane); that used in the afterburner was MIL-F-5624A grade JP-4.

RESULTS AND DISCUSSION

Operating Limits

The operating range of the afterburner at a flight Mach number of 0.8 is shown in figure 5. The maximum altitude obtainable was limited by the capacity of the test facilities; however, operation at an altitude of 55,000 feet was possible at only one fuel-air ratio, indicating this to be the maximum altitude limit. The trend of a decreasing fuel-air ratio range with increasing altitude substantiates the conclusion that the maximum operating altitude is in this region. The trend of decreasing rich fuel-air ratio with altitude is typical of most engines and is due to the maximum afterburner gas temperature obtainable with a constant-area (wide-open) jet nozzle that arises from the Reynolds number effect on component efficiencies. Operation at stoichiometric afterburner fuel-air ratio was possible up to an altitude of 45,000 feet. It is expected that operation would have been possible at this fuel-air ratio at altitudes up to 55,000 feet or above had it been possible to further increase nozzle-exit area.

Performance Characteristics

The performance data for several flight conditions are presented in tabular form (table I) and are shown graphically in figures 6 through 9. The variations in combustion temperature and efficiency with afterburner fuel-air ratio are presented in figure 6. Performance data at an altitude of 45,000 feet and a flight Mach number of 0.8 were obtained at afterburner fuel-air ratios greater than the operational range (fig. 5). These data were obtained to more definitely establish the combustion temperature at stoichiometric fuel-air ratio by allowing the afterburner-inlet temperature to exceed 1625° R. Both the combustion temperature and efficiency were in good agreement with the data of reference 1, which are shown by the dashed line in figure 6.

A peak combustion temperature of 3900° R and a corresponding efficiency of 0.96 were obtained at flight conditions corresponding to afterburner-inlet pressures from 2540 to 2800 pounds per square foot. Peak temperatures occurred at about stoichiometric fuel-air ratio (0.0675) for all conditions except the highest pressure levels, where the peak temperature occurred at a richer mixture. Combustion efficiency (fig. 6(b)) reached a maximum value at a fuel-air ratio of about 0.055 and remained relatively constant with increasing fuel-air ratio. The efficiency decreased with increasing altitude (decreasing afterburner-inlet pressure) with a resultant reduction in combustion temperature. This typical trend of efficiency with pressure is shown in figure 7 for a fuel-air ratio of 0.052. As shown in this figure, a reduction in burner-inlet pressure from 3090 to 510 pounds per square foot lowered the efficiency from 0.95 to 0.61 with a resultant reduction in combustion temperature from 3560° to 2880° R.

This afterburner configuration produced smooth combustion under all flight conditions tested; however, the similar configuration of reference 1 was subject to a buzzing condition very near the lean blow-out fuel-air ratio at an afterburner-inlet pressure of about 2450 pounds per square foot. Lean blow-out was not obtained at this afterburner-inlet pressure with the configuration of this investigation, but operation at a low fuel-air ratio was obtained without encountering a buzzing condition. Combustion was also stable at a fuel-air ratio as low as 0.027 at an afterburner-inlet pressure of 3090 pounds per square foot.

The pressure losses in an afterburner must also be considered in a complete evaluation of afterburner performance. The variation of afterburner pressure loss ratio with afterburner fuel-air ratio is presented in figure 8. The friction total-pressure loss for the cold burner was 6 percent of the afterburner-inlet pressure. The pressure loss ratio increased with increasing fuel-air ratio because of the momentum pressure loss. The pressure loss with afterburning at the stoichiometric fuel-air ratio was about double the friction loss for the cold burner. There was no apparent trend of pressure loss ratio with flight condition or afterburner-inlet pressure.

The effectiveness of the afterburner in terms of thrust is shown in figure 9(a) for the augmented jet thrust ratio and in figure 9(b) for the augmented net thrust ratio. The afterburner produced an augmented jet thrust ratio as high as 1.625 at an afterburner fuel-air ratio of 0.076 at the higher afterburner-inlet pressure levels which correspond to an augmented net thrust ratio of 2.03 at an altitude of 25,000 feet and a flight Mach number of 0.92. At lower pressure levels, the additional gain in augmented jet thrust obtained as the fuel-air ratio was increased above about 0.06 was small. The maximum augmented jet thrust ratio decreased with decreasing afterburner-inlet pressure as a result of the corresponding reductions in exhaust-gas temperature. Augmented jet thrust ratios greater than those measured may have been obtainable at altitudes of 50,000 and 55,000 feet by using a larger exhaust nozzle.

Effect of Fuel Distribution

At an altitude of 45,000 feet and a flight Mach number of 0.8, the fuel manifold pressure had decreased to approximately 25 pounds per square inch absolute at the stoichiometric fuel-air ratio. An attempt was made to improve the fuel penetration at this flight condition through increasing the fuel manifold pressure to 75 pounds per square inch absolute by using only the 12 long spray bars. A comparison of performance with the two fuel system configurations is presented in figure 10. Using only the 12 long spray bars resulted in a shift of the fuel-air ratio required for peak efficiency from 0.060 to about 0.100, with a resultant shift in fuel-air ratio for maximum combustion temperature from 0.068 to 0.078. The trends of increasing combustion efficiency of the 12 long spray bar configuration and the sustained efficiency of the 24 fuel spray bar configuration with increasing fuel-air ratio above

the stoichiometric mixture are unique with the method of calculating the efficiency. The efficiency, as defined in the appendix, is based on the ideal temperature rise which decreases above the stoichiometric mixture because of chemical energy remaining in the products of an ideal combustion. The most important effect of reducing the number of spray bars was the reduction in maximum temperature from 3420° to 3000° R. Penetration was insignificant in either case and the decrease in performance at a given fuel-air ratio was a result of circumferential and radial maldistribution. These results indicate the importance of providing a good fuel distribution in the afterburner and that such a distribution can be obtained only by using a large number of injection points rather than relying on penetration of the fuel jets into the air stream.

Fuel-Air Ratio Distribution

The fuel distribution was optimized in reference 1 by use of a temperature ladder comprising a 1/2-inch water-cooled Inconel tube spanning the diameter of the afterburner with pieces of 1/8-inch diameter welding rod of uniform length butt-welded to the tube. Local temperature profiles were observed by visual comparison of the color variations of the rods during afterburner operation. Since the criterion of a good fuel distribution system for the attainment of the maximum mean bulk gas temperature is a uniform fuel-air ratio distribution, in this investigation the fuel-air ratio distribution was checked during afterburner operation by direct measurement by use of a fuel-air ratio analyzer. Data from the fuel-air ratio analyzer using samples of the exhaust gas obtained from a survey at station 8, the exhaust-nozzle inlet, are presented in figure 11 for operation at an altitude of 35,000 feet and a flight Mach number of 1.0. The indicated fuel-air ratio distribution, which was fairly uniform, is an indication of the afterburner temperature profile that would be expected with this fuel system. Only a small additional increase in mean bulk temperature would be obtained near stoichiometric with a perfectly uniform fuel-air ratio profile (see fig. 6(a)).

Cooling-Air Requirements

In this investigation, the primary objective was to ascertain the performance over a wide range of flight conditions; the cooling air was therefore supplied from an outside source. The cooling-air flow supplied was adequate to permit operating with an allowable afterburner-shell temperature of 1550° F. During operation at an altitude of 35,000 feet and a flight Mach number of 1.0, the cooling-air requirements with parallel flow convective cooling were determined, and the data are presented in figure 12 as a function of combustion temperature for several average afterburner-shell temperatures. During this phase of the investigation the inlet cooling-air temperature was 83° F and the observed cooling-air temperature rise increased from 100° to 300° F as the combustion temperature was increased at a given average afterburner-shell temperature.

These data indicate that at the high combustion temperatures a large amount of cooling air was required for the convective system used herein. As much cooling air as 34 percent of the exhaust-gas flow was required to maintain an average afterburner-shell temperature of 1300° F at a combustion temperature of 3600° R. Minimizing the cooling-air flow requirements by increasing the average afterburner-shell temperature to the maximum safe operating temperature of the material is not representative of safe operation, since hot spots up to 250° F higher than the average were frequently encountered.

CONCLUDING REMARKS

An investigation was conducted to ascertain the operational limits of a high-temperature afterburner and to determine its performance over a wide range of flight conditions. Operational limits were obtained at a flight Mach number of 0.8 and performance data were obtained at altitudes from 10,000 to 55,000 feet and flight Mach numbers from 0.6 to 1.0.

The afterburner, designed to provide high combustion temperature, had a peak combustion temperature of 3900° R, representing a combustion efficiency of 0.96 and an augmented jet thrust ratio of 1.625 at an afterburner-inlet pressure of 2540 pounds per square foot. At these conditions, which compared with an altitude of 25,000 feet and a flight Mach number of 0.92, the augmented net thrust ratio was 2.03. A maximum operational altitude of 55,000 feet at a flight Mach number of 0.8 was obtained with an afterburner fuel-air ratio of 0.052. At this condition the combustion temperature was 2880° R, representing a combustion efficiency of 0.61. Maximum combustion efficiency was obtained at fuel-air ratios of about 0.055 and remained relatively constant with increasing fuel-air ratio. Peak combustion temperatures were obtained at the stoichiometric fuel-air ratio or at slightly richer mixtures.

The attainment of a high bulk gas temperature was dependent upon the attainment of a uniform fuel distribution. At an altitude of 45,000 feet and a flight Mach number of 0.8, the use of 24 instead of 12 spray bars resulted in an increase in temperature from 3000° to 3420° R and a decrease in fuel-air ratio for maximum temperature from 0.078 to 0.068.

A severe cooling-air requirement was imposed on the convective shell cooling system used during this investigation. As much cooling air as 34 percent of the exhaust-gas flow was required to maintain an average afterburner-shell temperature of 1300° F at a combustion temperature of about 3600° R, which stresses the need for a more effective method of utilizing the cooling air.

Lewis Flight Propulsion Laboratory
National Advisory Committee for Aeronautics
Cleveland, Ohio

APPENDIX - CALCULATIONS

Symbols

The following symbols are used in this report:

A	cross-sectional area, sq ft
C_T	coefficient of thermal expansion
$C_{v,e}$	effective velocity coefficient
F_J	jet thrust, lb
F_N	net thrust, lb
f/a	fuel-air ratio
g	acceleration due to gravity, 32.17 ft/sec^2
H^o	sum of sensible enthalpy and chemical energy, Btu/lb
M	flight Mach number
m	mass flow, slugs/sec
P	total pressure, lb/sq ft
p	static pressure, lb/sq ft
R	gas constant, $\frac{1546 \text{ ft-lb}}{(\text{molecular weight})\ (\text{lb})\ (^oR)}$
T	total temperature, ^oR
V	velocity, ft/sec
W_a	air flow, lb/sec
W_f	fuel flow, lb/hr
W_g	gas flow, lb/sec
γ	ratio of specific heats
η	combustion efficiency

λ^{o} a term accounting for difference between H^{o} of carbon dioxide and that of water vapor in burned mixture and H^{o} of oxygen removed from air by their formation

Subscripts:

a air

b afterburner

e engine

ef effective

g gas

m fuel manifold conditions

max maximum

n exhaust-nozzle throat

Numbered subscripts as indicated on fig. 1

Methods of Calculation

Gas flow. - Engine-inlet air flow was calculated from measurements at station 1 using the following equation:

$$W_{a,1} = A_1 \sqrt{\frac{g}{R_{a,1}}} \frac{p_1}{\sqrt{T_1}} \left(\frac{pA}{m\sqrt{gRT}} \right)_1^{-1} \tag{1}$$

Values of the static-pressure parameter $\frac{pA}{m\sqrt{gRT}}$ were obtained from reference 3 assuming $\gamma_{a,1}$ to be 1.4. The gas flows at the entrance and exit of the afterburner were then determined by adding the appropriate fuel flow to the engine-inlet air flow.

Afterburner fuel-air ratio. - The afterburner fuel-air ratio is defined as the ratio of the afterburner fuel flow plus the unburned fuel from the engine combustor corrected for the difference in heating value of the two fuels to the unburned air entering the afterburner:

$$\left(\frac{f}{a} \right)_b = \frac{W_{f,b} + 1.013\ (1-\eta_e)\ W_{f,e}}{3600\ W_{a,1} - \eta_e \frac{W_{f,e}}{0.0665}} \tag{2}$$

where 1.013 is the ratio of the lower heat of combustion of the engine fuel to that of the afterburner fuel and η_e is the ratio of the ideal to actual engine fuel flow required to heat the air flow from engine-inlet to afterburner-inlet temperature. The stoichiometric fuel-air ratio of the engine fuel is 0.0665.

Afterburner combustion temperature. - The combustion temperature was calculated from the gas flow and a pressure survey at station 8 using the continuity equation as follows:

$$T_8 = (A_8 C_T)^2 \frac{g}{R_{g,8}} \left(\frac{p_8}{W_{g,8}}\right)^2 \left(\frac{pA}{m\sqrt{gRT}}\right)_8^{-2} \tag{3}$$

Values of the static-pressure parameter were obtained in the same manner as for the engine-inlet air flow using appropriate values for $\gamma_{g,8}$. The gas constant, $R_{g,8}$, and $\gamma_{g,8}$ were determined from the products of ideal combustion with no dissociation using the weighted averaging process and based on values obtained from reference 4. A water-gas reaction constant of 3.8 was assumed for mixtures greater than stoichiometric. The area A_8 was measured at room temperature and C_T was assumed to be unity, since the area at station 8 was water-cooled.

Afterburner combustion efficiency. - The combustion efficiency is defined as the ratio of the increase in energy of the exhaust gases in the afterburner to the ideal energy increase based on the afterburner fuel flow and the unburned engine fuel flow entering the afterburner:

$$\eta_b = \frac{W_{g,8} H^\circ_{g,8} - W_{g,5} H^\circ_{g,5} - \frac{W_{f,b}}{3600} \lambda^\circ_{b,m}}{W_{g,8} H^\circ_{g,T_{max}} - W_{g,5} H^\circ_{g,5} - \frac{W_{f,b}}{3600} \lambda^\circ_{b,m}} \tag{4}$$

The term H° was determined in the same manner as the gas constant in the calculation of combustion temperature. The value of $H^\circ_{g,T_{max}}$ was determined from the ideal energy modified by an energy difference to account for the increase in chemical energy in the products of combustion due to the effect of dissociation. The value of this energy difference was based on data contained in reference 5.

Thrust. - The jet thrust was determined from the gas flow, the combustion temperature, and the ratio of exhaust-nozzle total pressure to altitude pressure P_8/p_0 by means of the following relations:

$$F_J = C_{v,e}\left[\frac{W_{g,8}}{g} V_n + A_n (p_n - p_0)\right] \tag{5}$$

$$F_J = C_{v,e} W_{g,8}\sqrt{\frac{R_{g,8} T_8}{g}}\left(\frac{V_{ef}}{\sqrt{gRT}}\right) \tag{6}$$

where

$$\frac{V_{ef}}{\sqrt{gRT}} = \frac{V_n}{\sqrt{gRT}} + \frac{p_n A_n}{m\sqrt{gRT}} - \frac{p_0 A_n}{m\sqrt{gRT}} \tag{7}$$

Values of the effective velocity parameter $V_{ef}/\sqrt{gRT}$ were obtained from reference 3 and the ratio of exhaust-nozzle total pressure to altitude pressure P_8/p_0 using appropriate values of $\gamma_{g,8}$.

The normal jet thrust (no afterburning) was calculated in a similar manner using the conditions of the exhaust gases at the turbine outlet (station 5) and a total-pressure loss of 6 percent of P_5 for the nonoperative afterburner. The effective velocity coefficient $C_{v,e}$ was assumed to be unity in both cases. The augmented jet thrust ratio was then obtained by dividing the jet thrust by the normal jet thrust.

The net thrust was calculated from the jet thrust and inlet momentum:

$$F_N = F_J - mV_0 \tag{8}$$

where

$$mV_0 = p_1 A_1 \left(\frac{pA}{m\sqrt{gRT}}\right)_1^{-1} \left(\frac{V}{\sqrt{gRT}}\right)_0 \tag{9}$$

Values of $(V/\sqrt{gRT})_0$ were based on the desired ram ratio assuming γ to be 1.4. Values of the static-pressure parameter were the same as those used to determine the engine air flow. The augmented net thrust ratio was then obtained by dividing the net thrust by the normal net thrust.

REFERENCES

1. Conrad, E. William, and Campbell, Carl E.: Altitude Wind Tunnel Investigation of High-Temperature Afterburners. NACA RM E51L07, 1952.

2. Gerrish, Harold C., Meem, J. Lawrence, Jr., Scadron, Marvin D., and Colnar, Anthony: The NACA Mixture Analyzer and Its Application to Mixture Distribution Measurement in Flight. NACA TN 1238, 1947.

3. Turner, L. Richard, Addie, Albert N., and Zimmerman, Richard H.: Charts for the Analysis of One-Dimensional Steady Compressible Flow. NACA TN 1419, 1948.

4. Huff, Vearl N., Gordon, Sanford, and Morrell, Virginia E.: General Method and Thermodynamic Tables for Computation of Equilibrium Composition and Temperature of Chemical Reactions. NACA Rep. 1037, 1951. (Supersedes NACA TN's 2161 and 2113.)

5. Mulready, Richard C.: The Ideal Temperature Rise Due to the Constant Pressure Combustion of Hydrocarbon Fuels. M.I.T. Meteor Rep. UAC-9, Res. Dept., United Aircraft Corp., July 1947. (BuOrd Contract NOrd 9845.)

TABLE I. - HIGH-TEMPERATURE AFTERBURNER PERFORMANCE

Data run	Altitude, ft	Flight Mach number, M_O	Afterburner fuel-air ratio, $(f/a)_b$	Engine-inlet temperature, T_1, °R	Engine-inlet pressure, P_1, lb/sq ft	Engine-inlet air flow, $W_{a,1}$, lb/sec	Engine speed, rpm	Engine fuel-air ratio, $(f/a)_e$	Engine combustion efficiency, η_e	Afterburner-inlet temperature, T_5, °R	Run
										24 spray bar fuel	
70-27	10,000	0.6	0.0271	546	1856	48.81	12,505	0.0148	1.00	1620	1
28			.0404	547	1860	48.79	12,502	.0148	1.00	1623	2
29			.0477	549	1855	48.42	12,509	.0148	1.01	1632	3
91-9	15,000	0.6	0.0331	503	1504	42.73	12,494	0.0158	0.99	1641	4
8			.0422	503	1507	42.99	12,486	.0157	.99	1631	5
7			.0556	502	1515	43.00	12,502	.0158	.98	1632	6
6			.0609	501	1506	42.95	12,494	.0157	.99	1629	7
5			.0704	501	1506	43.01	12,511	.0157	.99	1633	8
4			.0787	500	1510	43.18	12,509	.0159	.98	1626	9
70-32	25,000	0.6	0.0481	470	1000	29.32	12,502	0.0163	0.98	1631	10
33			.0600	466	1004	29.51	12,502	.0158	.98	1596	11
35			.0669	464	1003	29.55	12,503	.0162	.99	1630	12
34			.0720	466	1004	29.70	12,502	.0162	.99	1632	13
37			.0875	462	1000	29.57	12,489	.0164	.98	1633	14
36			.0939	463	1003	29.58	12,505	.0162	.99	1626	15
83-1	25,000	0.92	0.0385	506	1348	37.69	12,497	0.0157	0.99	1632	16
2			.0499	504	1355	37.97	12,505	.0156	.99	1631	17
3			.0630	505	1346	37.69	12,502	.0153	1.00	1622	18
4			.0750	504	1349	37.89	12,499	.0155	1.00	1634	19
58-6	35,000	1.0	0.0384	472	947	28.19	12,502	0.0164	0.95	1608	20
63-7			.0427	476	937	27.27	12,505	.0166	.94	1616	21
58-7			.0429	472	949	28.00	12,502	.0165	.94	1606	22
8			.0479	473	942	28.10	12,503	.0168	.96	1638	23
62-22			.0501	473	939	27.61	12,511	.0166	.96	1626	24
58-1			.0511	472	954	28.30	12,477	.0166	.97	1639	25
69-9			.0551	474	946	27.47	12,515	.0161	.98	1622	26
58-2			.0566	472	951	28.04	12,511	.0165	.97	1638	27
62-12			.0595	477	943	27.76	12,497	.0166	.96	1629	28
70-9			.0609	474	938	27.57	12,506	.0162	.98	1624	29
61-18			.0609	473	942	27.21	12,499	.0169	.94	1628	30
70-1			.0614	475	939	27.56	12,502	.0162	.97	1623	31
58-3			.0621	477	948	27.85	12,511	.0167	.95	1634	32
61-11			.0653	475	948	27.48	12,490	.0166	.95	1617	33
64-1			.0660	473	956	28.11	12,509	.0162	.97	1619	34
70-8			.0676	476	935	27.46	12,509	.0162	.98	1626	35
2			.0685	477	935	27.21	12,484	.0164	.96	1626	36
58-4			.0687	480	936	27.35	12,508	.0167	.95	1632	37
9			.0710	473	945	28.15	12,505	.0166	.96	1627	38
70-3			.0738	477	942	27.34	12,515	.0162	.97	1624	39
7			.0758	476	935	27.23	12,503	.0163	.97	1626	40
58-10			.0765	473	944	28.10	12,499	.0166	.96	1636	41
70-4			.0813	477	939	27.28	12,499	.0162	.98	1626	42
6			.0815	475	935	27.27	12,492	.0163	.97	1627	43
63-3			.0850	473	940	27.83	12,509	.0167	.96	1635	44
64-17			.0884	478	938	27.42	12,506	.0175	.93	1653	45
70-5			.0888	476	935	27.46	12,499	.0162	.98	1628	46
62-33	40,000	0.8	0.0333	420	594	18.70	12,508	0.0180	0.92	1620	47
58-16			.0392	436	592	18.53	12,502	.0180	.91	1628	48
17			.0438	436	596	18.60	12,497	.0175	.92	1607	49
18			.0505	436	593	18.33	12,508	.0178	.92	1621	50
19			.0573	436	593	18.10	12,511	.0178	.91	1616	51
20			.0634	436	593	18.10	12,512	.0179	.91	1615	52
21			.0679	436	591	18.29	12,514	.0180	.92	1636	53
84-4			.0710	443	601	18.03	12,500	.0167	.97	1624	54
11			.0731	443	589	17.82	12,480	.0172	.96	1637	55
58-11	45,000	0.8	0.0394	439	472	14.49	12,499	0.0180	0.89	1610	56
89-8			.0416	445	468	14.15	12,492	.0192	.87	1649	57
58-12			.0444	439	463	14.56	12,514	.0180	.91	1626	58
87-39			.0460	447	462	14.14	12,503	.0185	.90	1657	59
58-13			.0504	438	465	14.38	12,500	.0183	.89	1618	60
89-7			.0520	448	467	14.11	12,497	.0188	.87	1637	61
58-14			.0566	438	463	14.35	12,503	.0184	.88	1617	62
89-5			.0575	444	467	14.18	12,531	.0188	.87	1627	63
87-40			.0579	450	462	13.94	12,494	.0185	.89	1637	64
58-15			.0604	439	465	14.59	12,512	.0181	.91	1634	65
69-6			.0606	441	471	14.22	12,506	.0184	.88	1622	66
89-6			.0634	443	467	14.18	12,506	.0190	.87	1639	67
70-22			.0668	434	466	14.24	12,514	.0187	.89	1637	68
69-5			.0671	438	468	14.21	12,494	.0186	.88	1631	69
-7			.0690	440	475	14.30	12,443	.0185	.87	1613	70
62-28			.0693	450	465	13.98	12,500	.0185	.88	1624	71
84-9			.0726	443	459	13.89	12,500	.0181	.91	1638	72
8			.0739	444	459	13.94	12,500	.0180	.92	1644	73
69-8			.0787	440	467	13.69	12,487	.0190	.88	1649	74
62-31	50,000	0.8	0.0442	429	367	11.32	12,500	0.0192	0.84	1606	75
30			.0521	433	363	11.21	12,500	.0197	.84	1624	76
84-6			.0552	450	367	10.93	12,497	.0190	.86	1634	77
62-29			.0582	437	370	11.27	12,509	.0193	.86	1634	78
62-32	55,000	0.8	0.0522	465	288	8.52	12,518	0.0202	0.79	1622	79
										12 spray bar fuel	
59-10	45,000	0.8	0.0573	452	464	14.15	12,484	0.0184	0.87	1612	80
8			.0669	450	477	14.39	12,508	.0180	.90	1621	81
7			.0758	440	460	14.03	12,506	.0189	.86	1619	82
11			.0805	429	460	14.22	12,494	.0189	.86	1608	83
12			.0813	427	477	14.77	12,499	.0182	.90	1614	84
13			.0900	425	459	14.27	12,497	.0188	.86	1600	85
14			.0905	423	469	14.70	12,494	.0185	.88	1610	86
15			.0976	423	472	14.76	------	.0184	.89	1611	87

NACA

AT SEVERAL ALTITUDES AND FLIGHT MACH NUMBERS

Data run	Afterburner-inlet pressure, P_5, $\frac{lb}{sq\ ft}$	Afterburner combustion temperature, T_8, $^\circ R$	Afterburner combustion efficiency, η_b	Afterburner pressure loss ratio, $\frac{(P_5 - P_8)}{P_5}$	Jet thrust, F_J, lb	Augmented jet thrust ratio	Net thrust, F_N, lb	Augmented net thrust ratio	Run
injection system									
70-27	3074	2445	0.673	0.082	3578	1.241	2570	1.370	1
28	3109	3121	.861	.103	4048	1.394	3039	1.604	2
29	3077	3474	.931	.116	4196	1.460	3193	1.707	3
91-9	2788	2755	0.774	0.076	3610	1.325	2763	1.472	4
8	2793	3223	.896	.085	3936	1.440	3084	1.640	5
7	2806	3508	.866	.093	4130	1.512	3279	1.743	6
6	2790	3744	.936	.100	4255	1.561	3406	1.815	7
5	2773	3810	.926	.107	4312	1.583	3462	1.847	8
4	2824	3885	.960	.119	4444	1.615	3591	1.891	9
70-32	----	3288	0.851	-----	2706	-----	----	-----	10
33	----	3593	.887	-----	2799	-----	----	-----	11
35	----	3678	.882	-----	2902	-----	----	-----	12
34	----	3623	.859	-----	2910	-----	----	-----	13
37	----	3500	.883	-----	2923	-----	----	-----	14
36	----	3403	.890	-----	2911	-----	----	-----	15
83-1	2532	2937	0.792	0.104	3765	1.366	2657	1.603	16
2	2538	3485	.917	.116	4150	1.496	3045	1.824	17
3	2531	3829	.960	.122	4357	1.586	3259	1.976	18
4	2577	3940	.972	.122	4534	1.626	3431	2.036	19
58-6	1807	2959	0.819	0.090	2957	1.390	2105	1.651	20
63-7	1768	3061	.805	.100	2899	1.411	2071	1.688	21
58-7	1806	3143	.851	.095	3029	1.437	2182	1.729	22
8	1829	3259	.835	.094	3132	1.456	2282	1.754	23
62-22	1780	3232	.796	.107	3031	1.450	2196	1.750	24
58-1	1836	3434	.885	.101	3230	1.494	2374	1.818	25
69-9	1735	3461	.858	.112	3093	1.505	2261	1.850	26
58-2	1827	3584	.900	.105	3278	1.532	2430	1.882	27
62-12	1783	3491	.836	.112	3185	1.515	2341	1.861	28
70-9	1745	3593	.876	.120	3182	1.535	2347	1.894	29
61-18	1773	3642	.898	.116	3181	1.546	2357	1.910	30
70-1	1754	3564	.862	.120	3174	1.529	2339	1.885	31
58-3	1820	3638	.889	.108	3288	1.549	2442	1.914	32
61-11	1777	3637	.872	.118	3216	1.554	2383	1.926	33
64-1	1804	3678	.888	.115	3320	1.566	2470	1.943	34
70-8	1748	3619	.852	.125	3200	1.548	2366	1.916	35
2	1744	3649	.881	.120	3210	1.566	2383	1.948	36
58-4	1785	3636	.861	.114	3238	1.558	2404	1.931	37
9	1817	3548	.830	.116	3307	1.545	2455	1.905	38
70-3	1746	3581	.846	.132	3188	1.553	2357	1.929	39
7	1747	3631	.868	.128	3219	1.569	2392	1.953	40
58-10	1826	3516	.828	.117	3326	1.547	2475	1.904	41
70-4	1749	3530	.858	.136	3197	1.558	2368	1.935	42
6	1749	3538	.862	.132	3210	1.562	2383	1.939	43
63-3	1792	3380	.830	.133	3240	1.530	2398	1.881	44
64-17	1779	3488	.881	.126	3264	1.557	2429	1.925	45
70-5	1751	3363	.850	.134	3187	1.538	2353	1.901	46
62-33	1189	2703	0.758	0.098	1750	1.311	1310	1.464	47
58-16	1176	2860	.748	.097	1788	1.352	1344	1.531	48
17	1166	3068	.802	.107	1846	1.409	1400	1.618	49
18	1170	3261	.815	.109	1891	1.454	1452	1.684	50
19	1163	3444	.839	.115	1918	1.498	1484	1.754	51
20	1160	3535	.847	.118	1946	1.523	1512	1.791	52
21	1175	3508	.815	.121	1980	1.513	1542	1.770	53
84-4	1125	3352	.760	.142	1844	1.472	1408	1.723	54
11	1141	3547	.836	.138	1917	1.519	1486	1.788	55
58-11	898	2755	0.686	0.107	1339	1.330	991	1.505	56
89-8	891	3028	.802	.112	1372	1.376	985	1.615	57
58-12	890	2869	.681	.105	1387	1.407	1037	1.545	58
87-39	947	3043	.748	.113	1424	1.381	1081	1.571	59
58-13	898	3149	.761	.119	1438	1.425	1093	1.646	60
89-7	878	3333	.829	.124	1432	1.454	1045	1.747	61
58-14	895	3252	.756	.125	1459	1.450	1114	1.685	62
89-5	874	3447	.835	.132	1460	1.480	1073	1.791	63
87-40	864	3320	.772	.134	1406	1.444	1067	1.682	64
58-15	903	3213	.717	.122	1486	1.442	1135	1.669	65
69-6	866	3391	.796	.128	1446	1.478	1103	1.738	66
89-6	874	3409	.786	.133	1458	1.474	1071	1.779	67
70-22	871	3402	.741	.138	1443	1.454	1102	1.691	68
69-5	876	3401	.767	.142	1458	1.475	1117	1.726	69
69-7	881	3391	.770	.139	1464	1.487	1120	1.749	70
62-28	877	3441	.788	.140	1453	1.493	1113	1.758	71
84-9	871	3368	.768	.141	1437	1.473	1101	1.720	72
8	876	3347	.763	.142	1445	1.469	1108	1.714	73
69-8	854	3365	.792	.122	1411	1.488	1081	1.747	74
62-31	691	2845	0.676	0.119	1057	1.344	788	1.524	75
30	683	3049	.695	.129	1085	1.386	817	1.585	76
84-6	668	3072	.677	.153	1033	1.369	767	1.570	77
62-29	684	3145	.695	.145	1094	1.396	824	1.605	78
62-32	510	2888	0.611	0.141	773	1.334	562	1.525	79
injection system									
59-10	883	2696	0.497	0.110	1311	1,330	966	1.509	80
8	905	2967	.581	.115	1405	1.401	1055	1.642	81
7	887	2995	.649	.115	1407	1.428	1069	1.652	82
11	888	2933	.668	.117	1421	1.428	1083	1.647	83
12	915	2912	.664	.106	1477	1.431	1127	1.653	84
13	902	2956	.744	.123	1462	1.458	1124	1.690	85
14	914	2930	.741	.121	1497	1.449	1150	1.677	86
15	920	2859	.767	.119	1505	1.449	1157	1.678	87

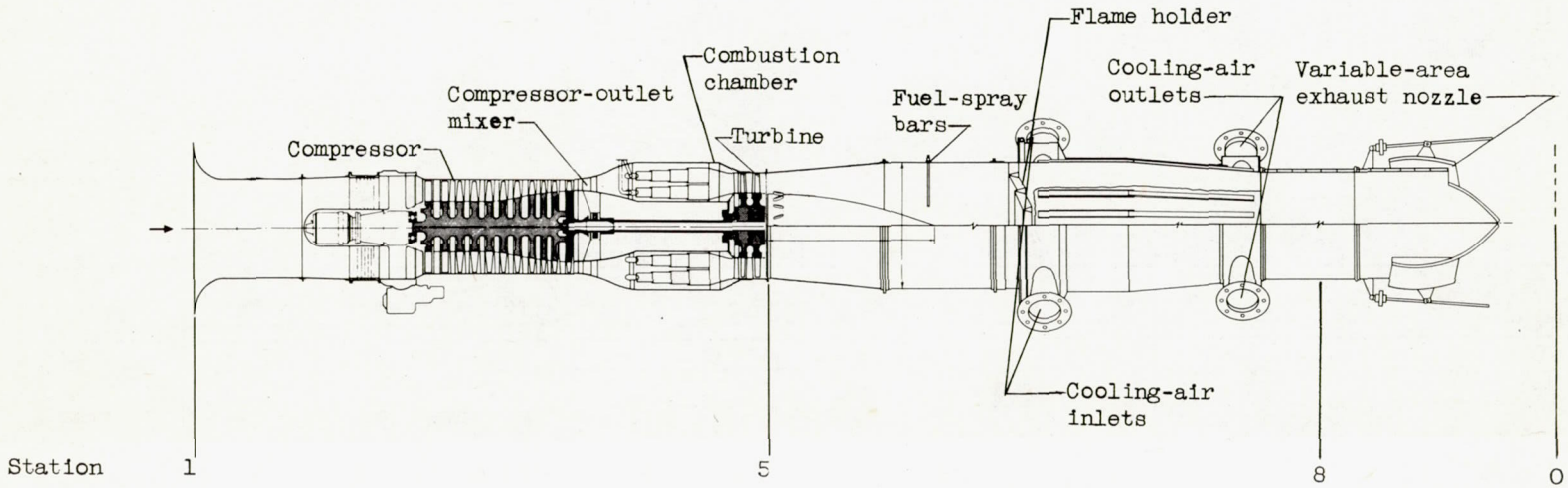

Station	1	5	8	0
Total-pressure probes	22	20	16	-
Static-pressure probes	9	4	8	5
Thermocouples	21	48	-	-

Figure 1. - Sectional view of engine showing instrumentation stations.

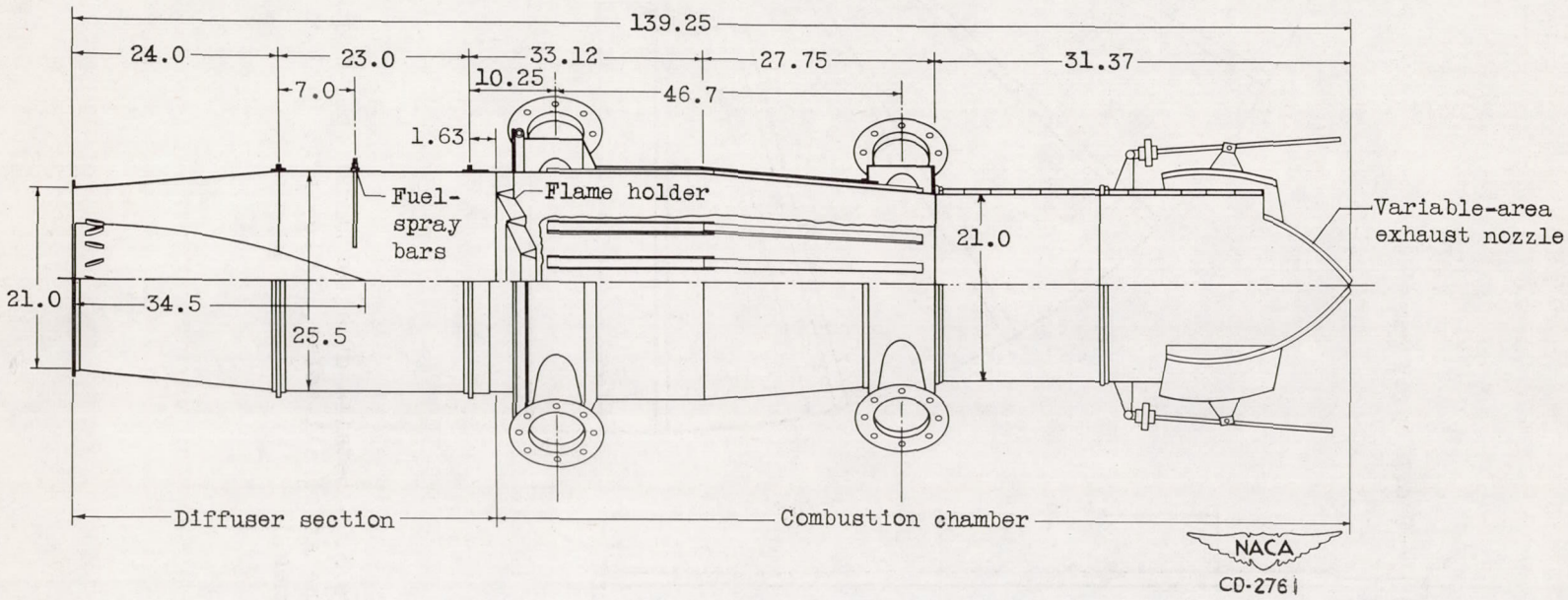

Figure 2. - Sectional view of afterburner. (All dimensions are in inches.)

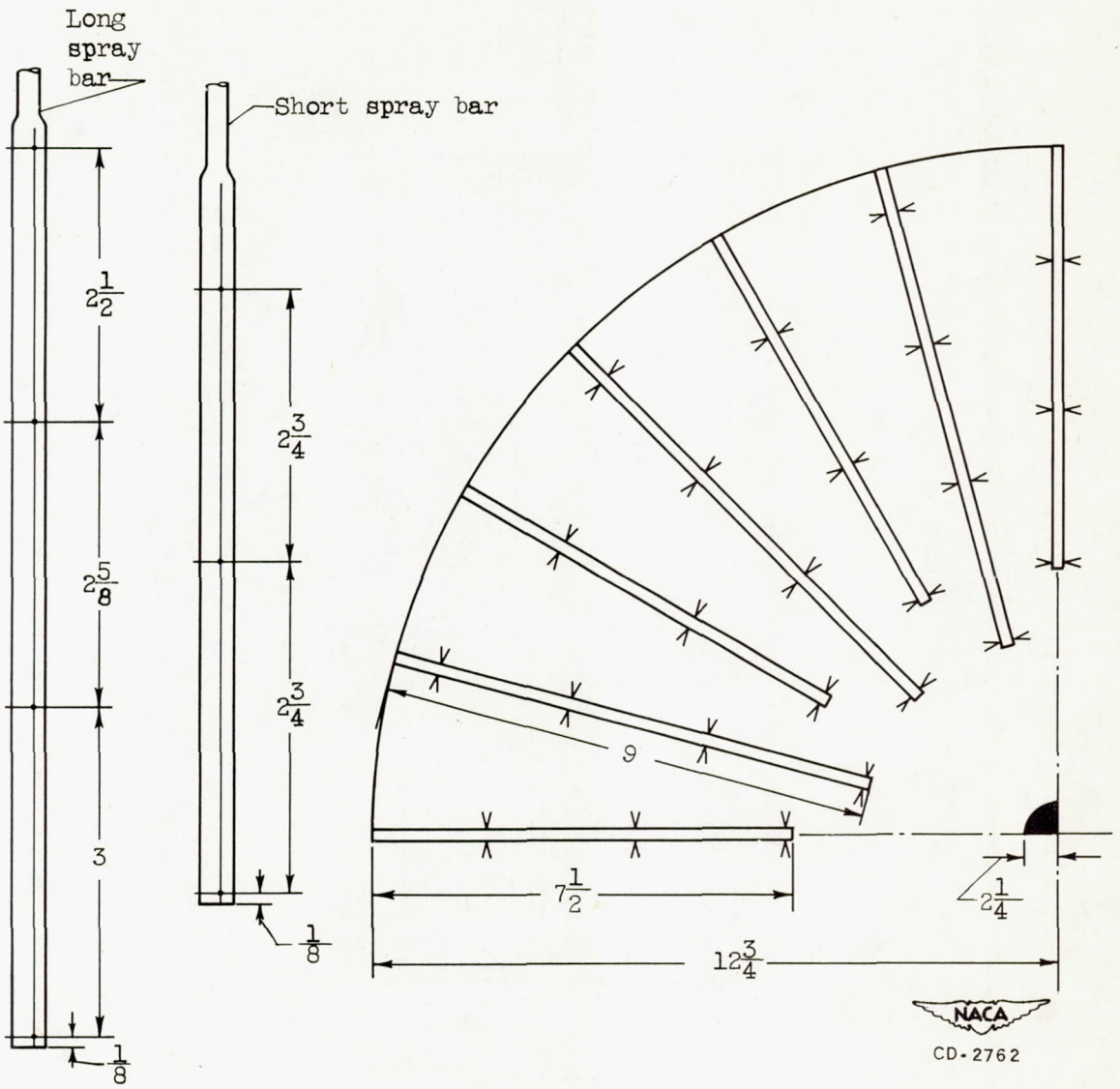

Figure 3. - Details of afterburner fuel-distribution system. Diameter of all holes, 0.020 inch. (All dimensions are in inches.)

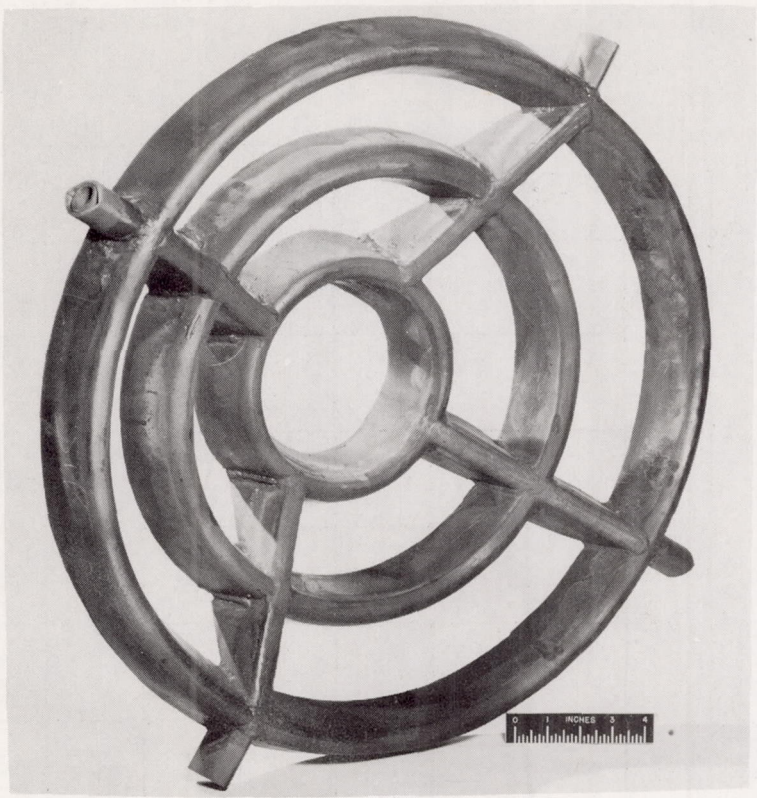

(a) View of flame holder.

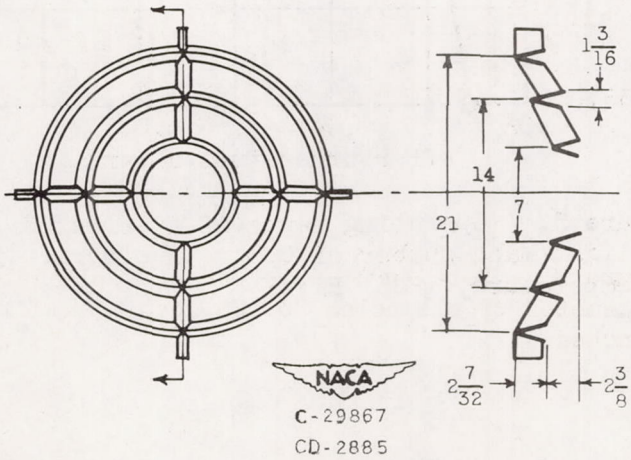

(b) Flame-holder dimensions. (All dimensions are in inches.)

Figure 4. - Details of afterburner flame holder. Area blockage, 35 percent.

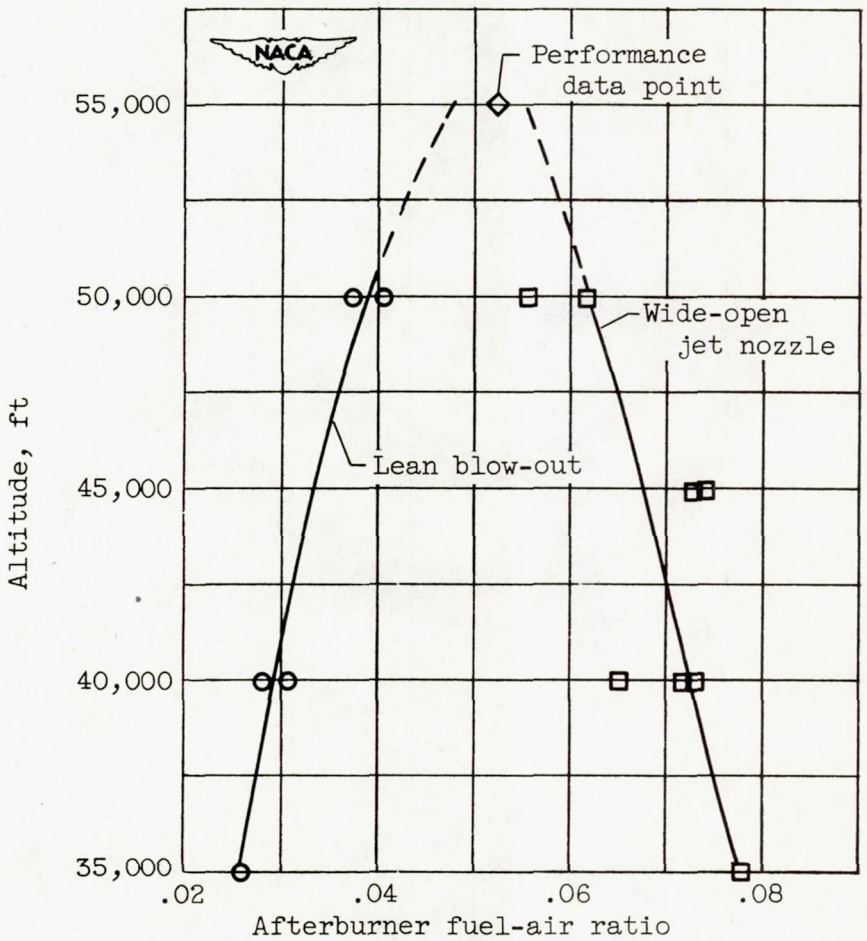

Figure 5. - Operating range of afterburner at flight Mach number of 0.8. Afterburner inlet temperature, 1625° R.

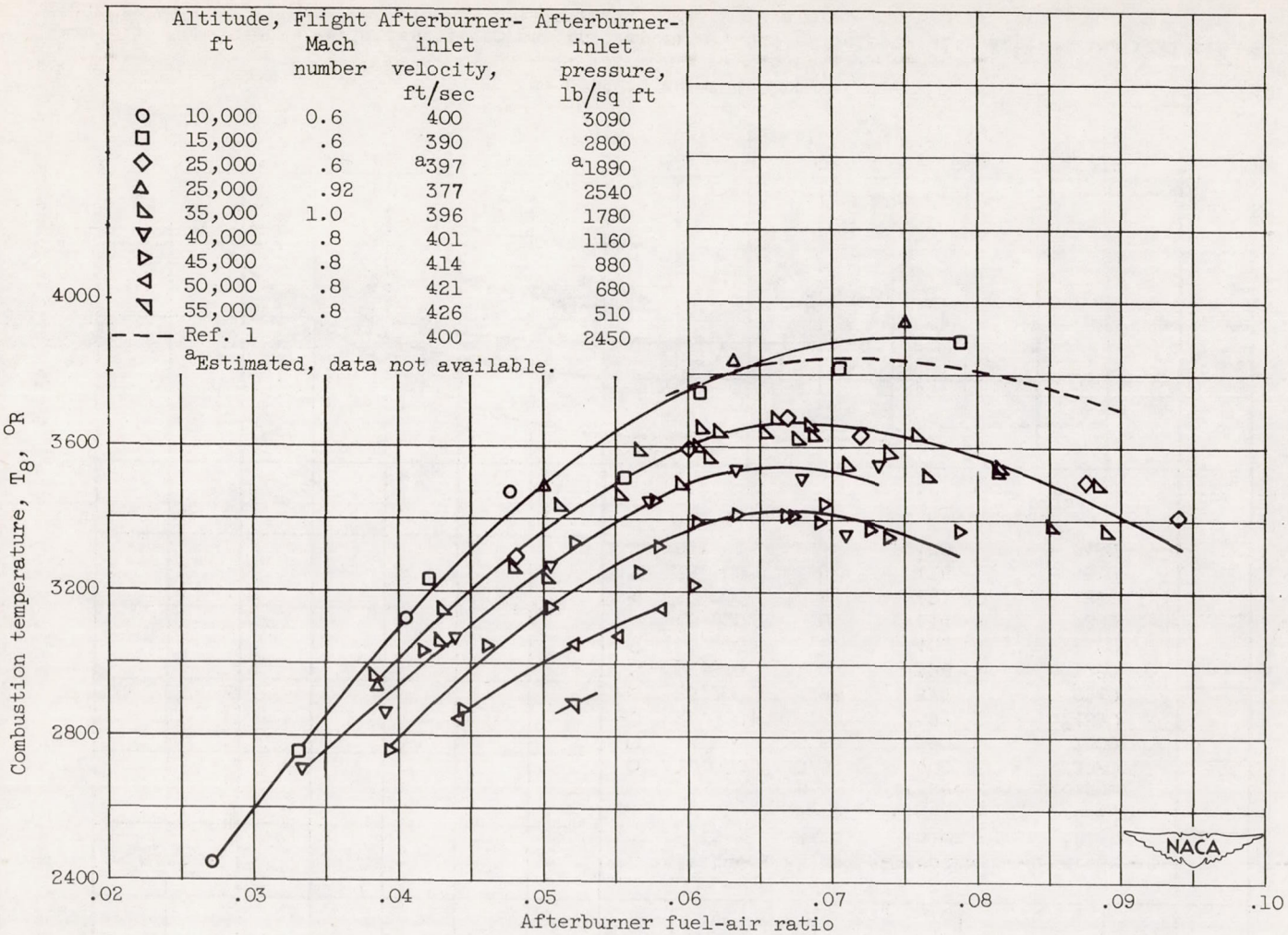

(a) Combustion temperature.

Figure 6. - Variation of combustion temperature and efficiency with afterburner fuel-air ratio at several flight conditions. Afterburner-inlet temperature, 1625° R.

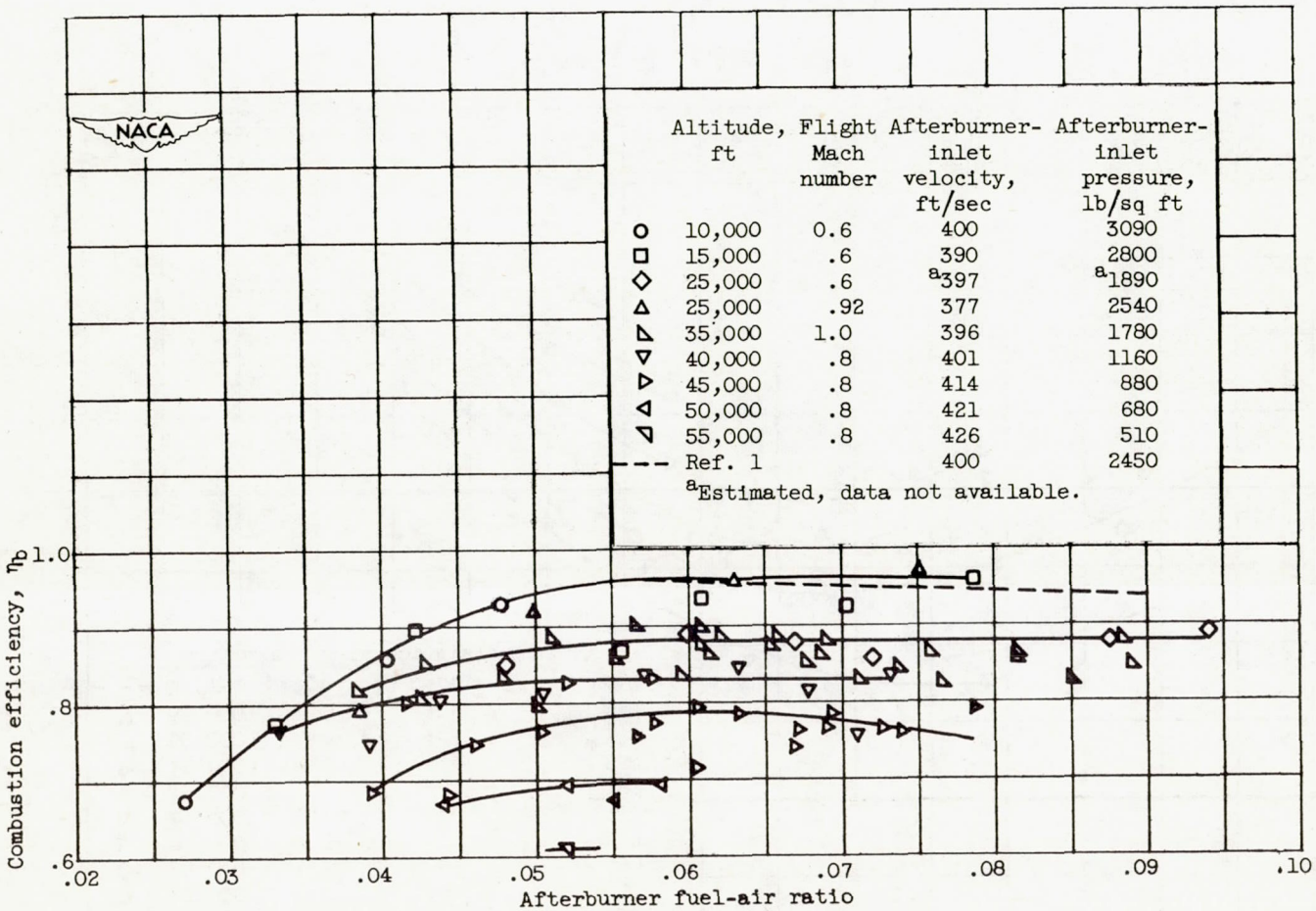

(b) Combustion efficiency.

Figure 6. - Concluded. Variation of combustion temperature and efficiency with afterburner fuel-air ratio at several flight conditions. Afterburner-inlet temperature, 1625° R.

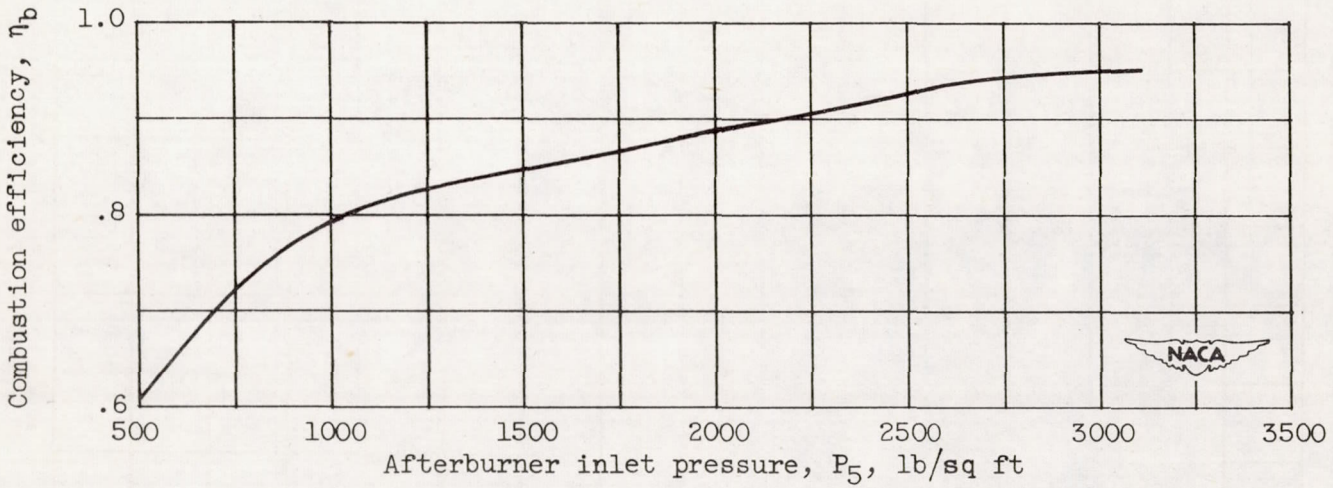

Figure 7. - Variation of combustion efficiency with afterburner-inlet pressure. Afterburner fuel-air ratio, 0.052; afterburner-inlet temperature, 1625° R.

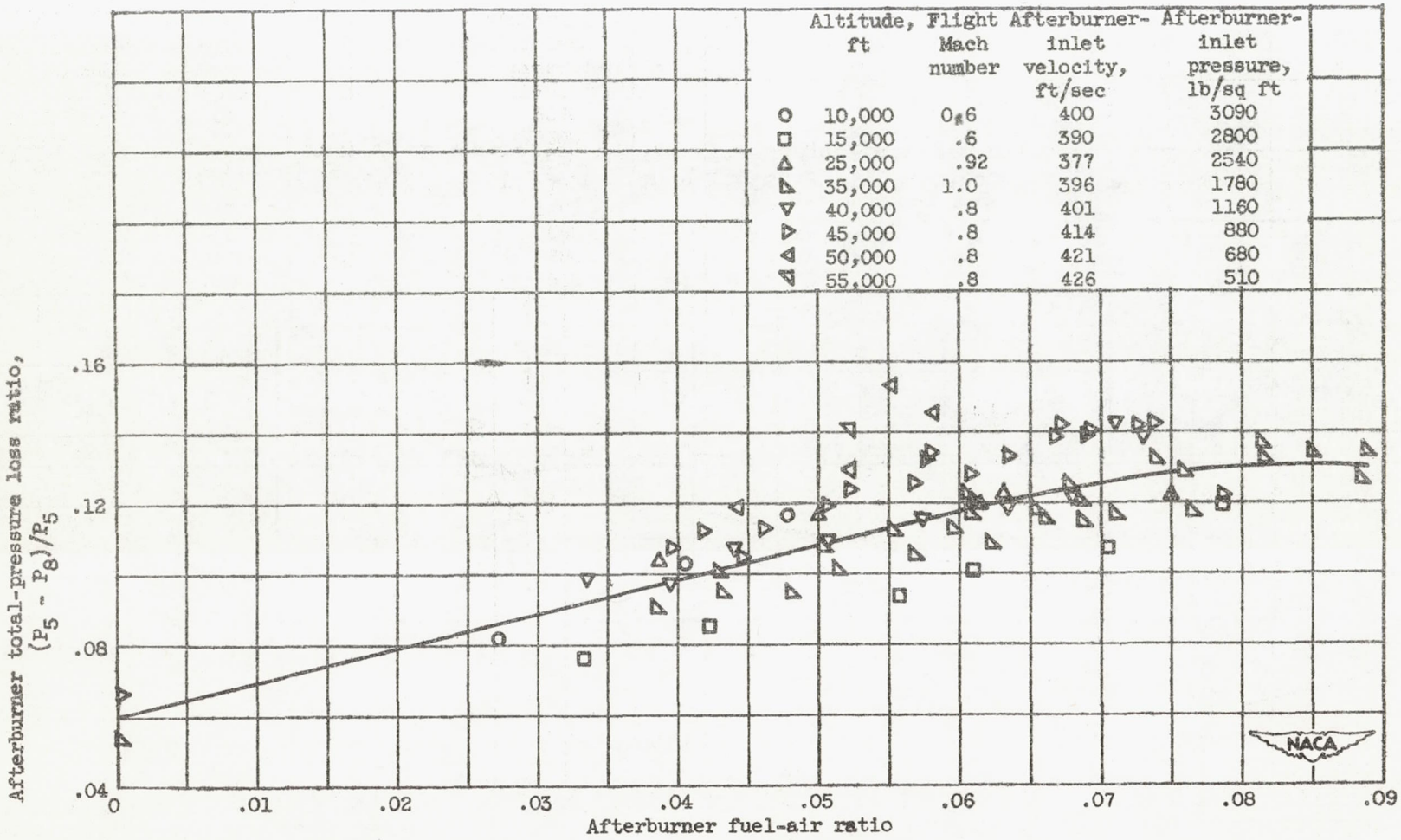

Figure 8. - Variation of afterburner total-pressure loss ratio with afterburner fuel-air ratio at several flight conditions.

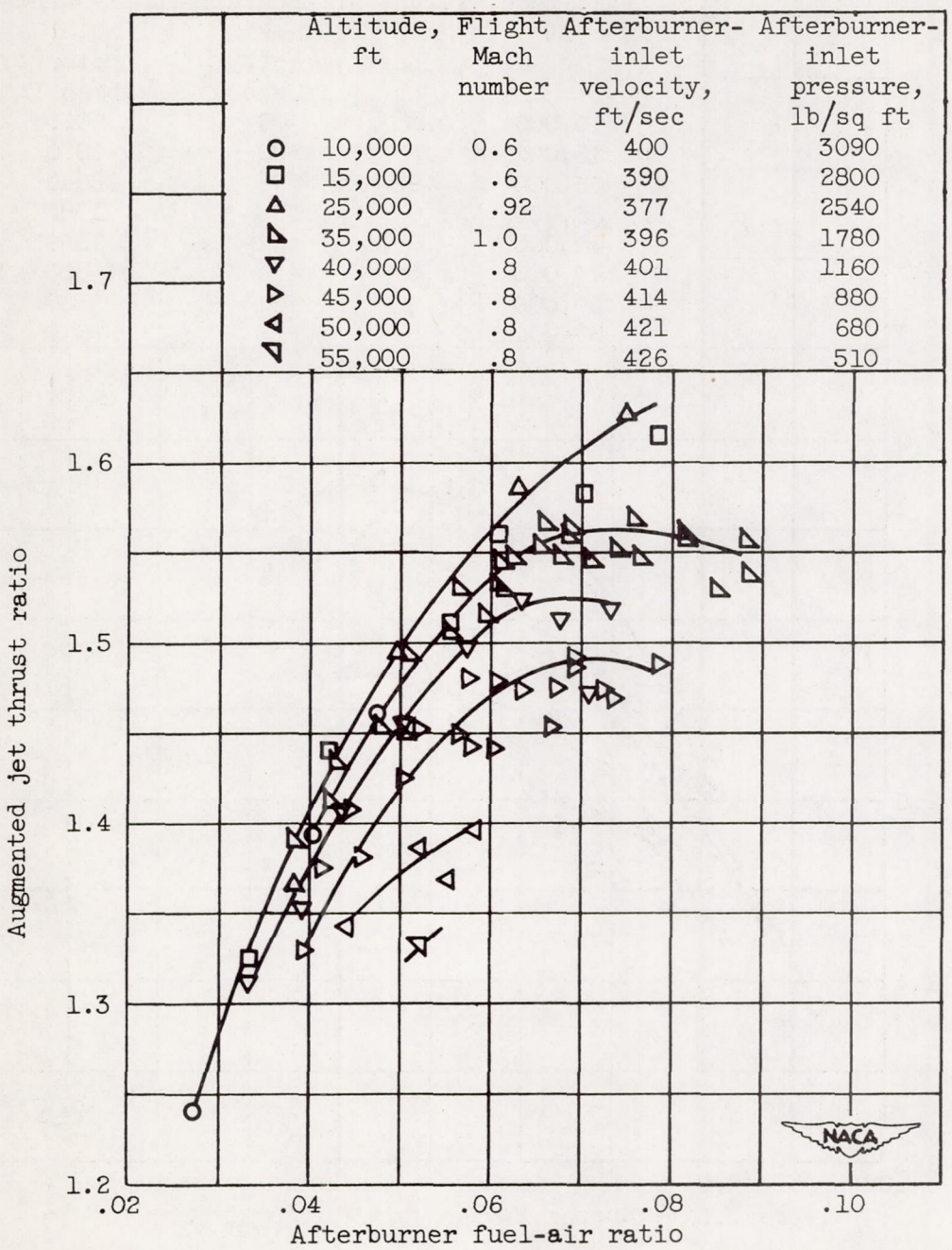

(a) Jet thrust.

Figure 9. - Variation of augmented thrust ratio with afterburner fuel-air ratio at several flight conditions.

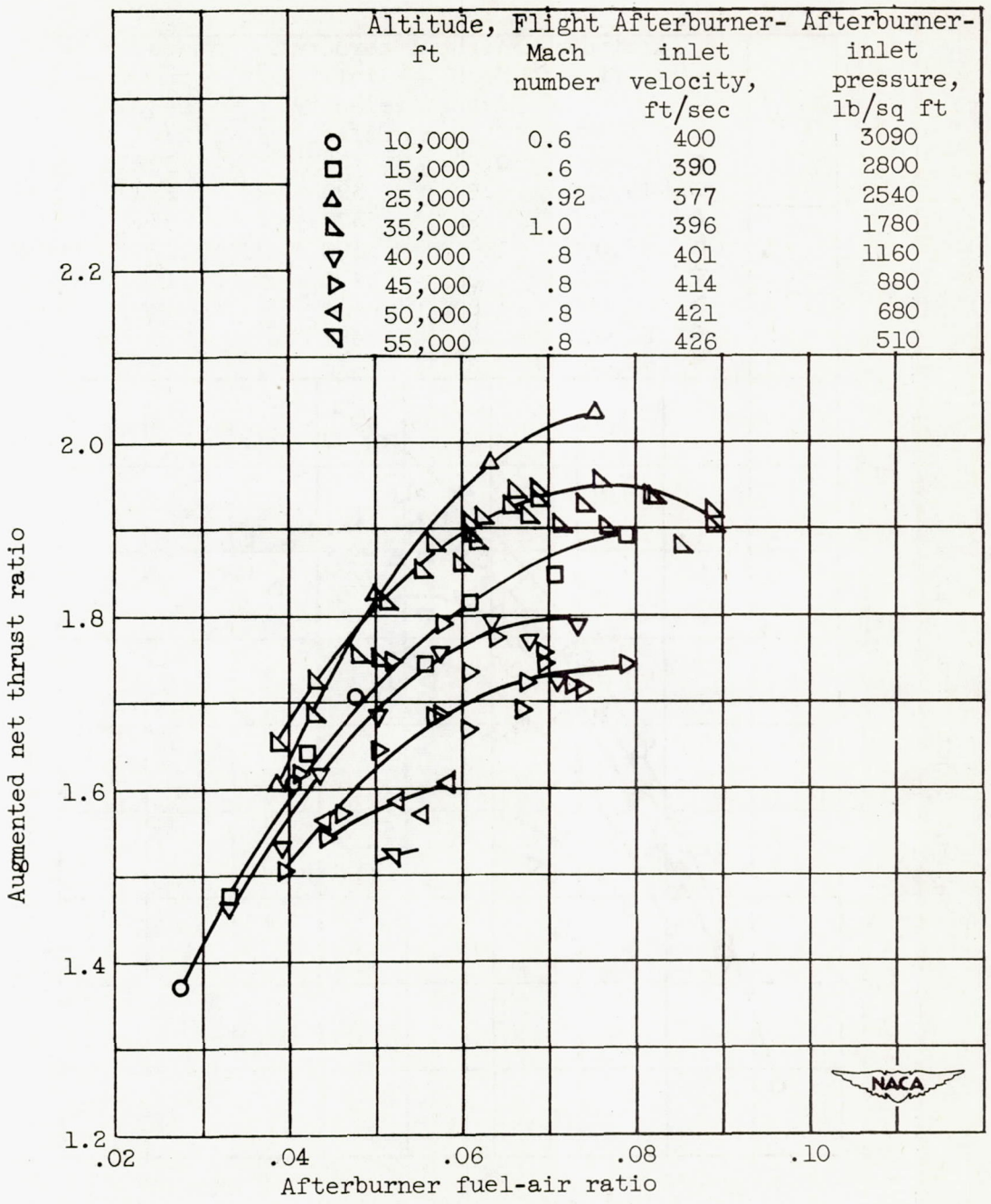

(b) Net thrust.

Figure 9. - Concluded. Variation of augmented thrust ratio with afterburner fuel-air ratio at several flight conditions.

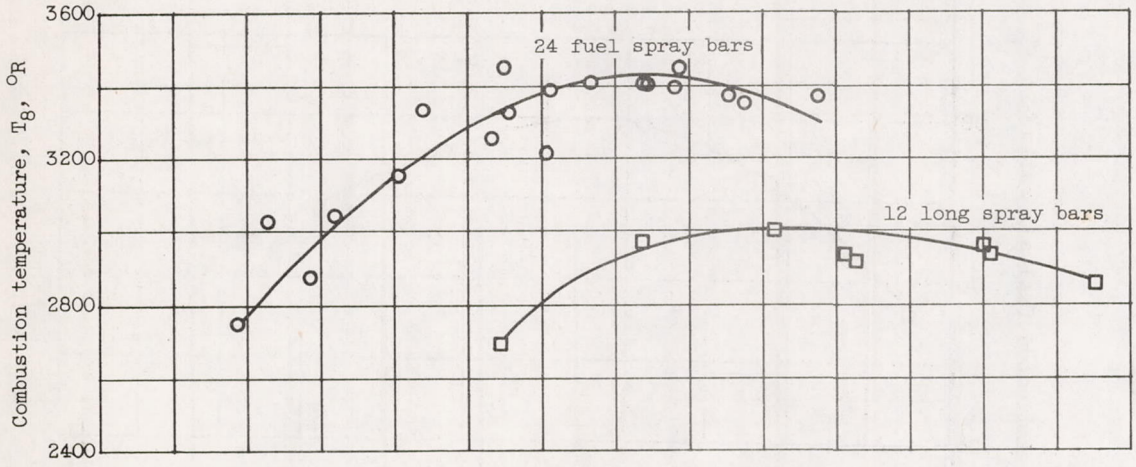

(a) Combustion temperature.

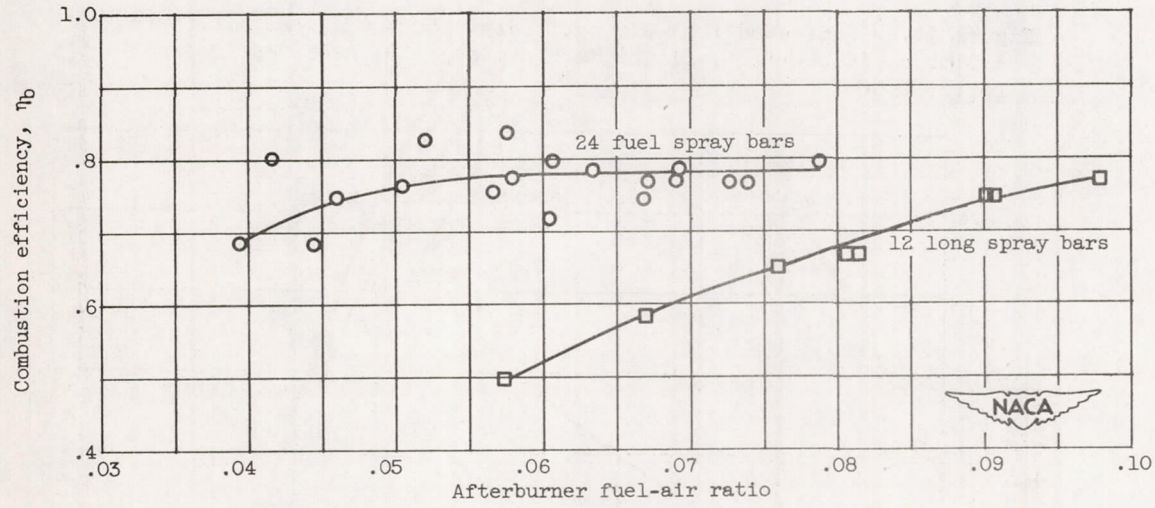

(b) Combustion efficiency.

Figure 10. - Variation of combustion temperature and efficiency with afterburner fuel-air ratio for two fuel system configurations. Altitude, 45,000 feet; flight Mach number, 0.8.

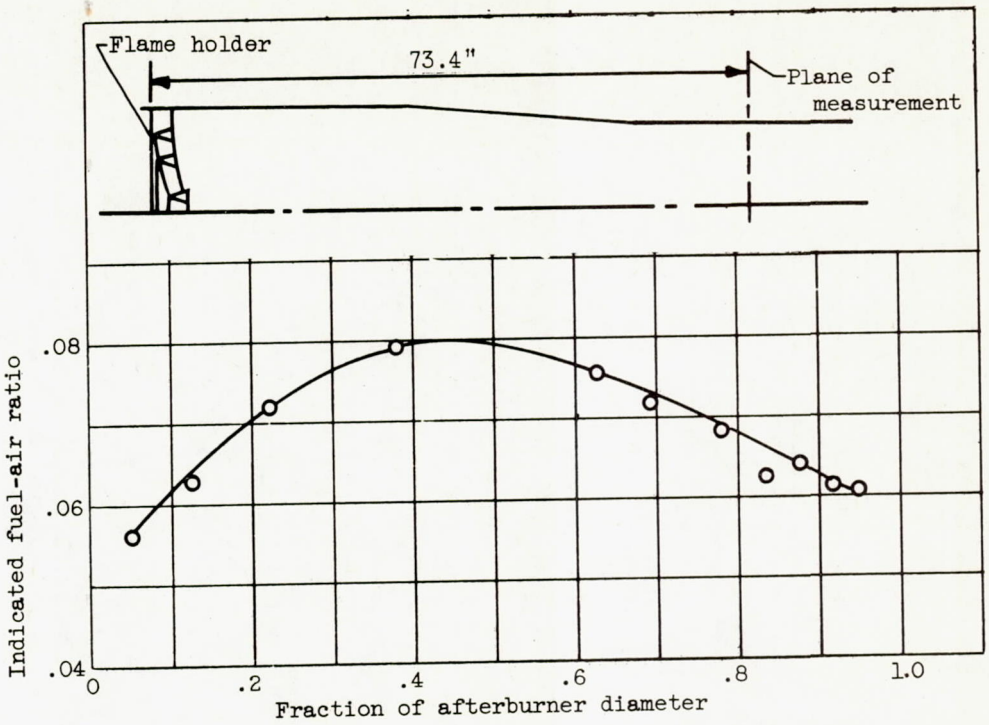

Figure 11. - Indicated fuel-air ratio distribution across afterburner. Altitude, 35,000 feet; flight Mach number, 1.0; measured fuel-air ratio, 0.069.

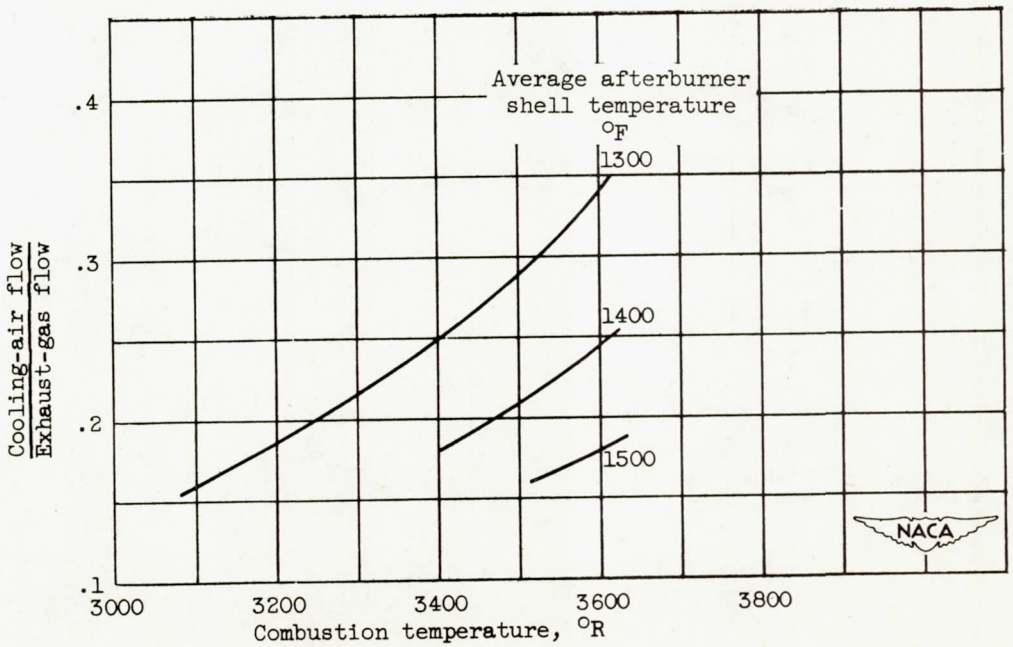

Figure 12. - Parallel flow cooling-air requirements of high-temperature afterburner. Altitude, 35,000 feet; flight Mach number, 1.0; inlet cooling-air temperature, 83° F; cooling-air temperature rise, 100-300° F.